CrossMark

# Study on the dual-curing mechanism of epoxy/allyl compound/sulfur system

Qingsong Lian[1], Yan Li[1], Tao Yang[1], Kai Li[1], Yifen Xu[2], Liang Liu[1], Jingbo Zhao[1], Junying Zhang[1,*], and Jue Cheng[1,*]

[1] *Key Laboratory of Carbon Fiber and Functional Polymers, Ministry of Education, Beijing University of Chemical Technology, Beijing 100029, People's Republic of China*
[2] *Aerospace Research Institute of Materials and Processing Technology, Beijing 100076, People's Republic of China*

## ABSTRACT

Allyl-based epoxy resin/Sulfur (S) system is a facile and novel dual-curing system which conducts a unique curing mechanism. In this paper, Bisphenol-A diglycidyl ether (BADGE) and 2-Allylphenol (OAP) cured by S were comparatively investigated to clarify the dual-curing mechanism of Epoxy (EP)/Allyl Compound (AC)/S system. When the temperature was above 170 °C, DSC and FTIR data showed that S could cleave to form thiyl radicals, and FTIR, NIR, and $^{1}$H NMR measurements proved the disappearance of allyl groups and the generation of thiol groups by the thiyl radicals abstracting α-H atoms of allyl groups in the OAP/S reaction system. Real-time infrared spectroscopy (RT-FTIR) results showed that the reaction of the generation of thiol groups is the dominant reaction in the two possible pathways of the OAP/S system; allyl groups and epoxy groups disappeared sequentially in the OAP/S/BADGE system. DSC curve also revealed the one-stage reaction for OAP/S system and two-stage reaction for OAP/S/ BADGE system. These data were used to develop a detailed, experimentally validated pathway for the dual-curing of EP/AC/S system, in which thiol groups are important intermediate, and the dual-curing process included the crosslinking of double bonds that initiated by thiyl radicals and the ring-opening reaction of epoxy groups with thiol groups. Besides, the dual-curing mechanism of EP/AC/S system shares a close resemblance to the classical rubber vulcanization mechanism and the recent thiol-ene radical addition mechanism.

## Introduction

Epoxy-based thermosets exhibit excellent mechanical properties, good dimensional stability, and wonderful heat resistance due to their irreversible three-dimensional (3-D) cross-linked networks after curing. Consequently, the curing mechanism of epoxy resins has been a research focus since its advent in the late 19$^{th}$ century. There are many factors determining the curing behavior including the structure of epoxy

Address correspondence to E-mail: zhangjy@mail.buct.edu.cn; chengjue@mail.buct.edu.cn

Springer

resin, the curing agents, and the curing methods [1–7]. In general, the curing reaction of epoxy resin is proceeding according to a single mechanism, which in many cases, however, cannot satisfy the demand with the development of the science and technology [8, 9]. Thus, dual-cured epoxy systems have provoked a great deal of interest.

Dual-curing is a technic that monomers are cross-linked in two types of sequential reactions [10, 11]. The interest in such complex curing processes is mainly due to its processing advantages, such as (a) dealing with the difference between the application date and bonding date; (b) application at one location and assembly at the other location; and (c) automated in line processes assembly [12].

Traditionally, a dual-cured epoxy system was constructed by mixing an epoxy resin with some other monomers with various groups together [13], such as acrylate [14], silicon [15], and aliphatic acid [16]. And in this way, the two different curing methodologies can be combined in one hybrid system, mostly being photo curing followed by thermal curing [17, 18]. In this case, the property of the curing products might be affected by the phase separation due to the poor compatibility. To solve this problem, a new thought is based on the synthesis of dual-functional epoxy resins, which contain two types of functional groups in one backbone. In this way, curing agents can react with the dual-functional epoxy resins in two different curing mechanisms [19]. However, to the best of our knowledge, reports about this kind of dual-curing are few because of the rare species of dual-functional epoxy resins. Furthermore, the two curing reactions carried out by different functional groups might inhibit with each other so that the degree of conversion could not reach a high level, which would influence the properties of the final curing products.

Among the dual-functional epoxy resins, diglycidyl ether of 4,4′-diallyl bisphenol-A (DADGEBA, see Fig. 1) is attractive due to its facile synthesis [20] and high reactivity [21]. Having both two allyl groups and two epoxy groups within one molecule, DADGEBA and its analogs such as 4,4′-(1-methylethylidene) bis(2-allylphenol) (DABPA) can be used to modify unsaturated resins [22] and bismaleimide (BMI) [23] to improve their mechanical properties. However, reports on the dual-curing of DADGEBA are rare. Our team found that DADGEBA could be cured by sulfur (S) [24], which is a novel
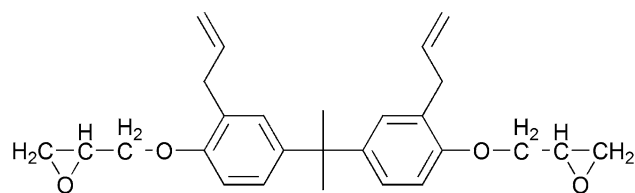


**Figure 1** The structure of DADGEBA.

curing agent that had never been reported for the curing of common epoxy thermosets in the previous research. And a more notable fact was that the degree of conversion of both the double bonds and epoxy groups could reach 100 % after the reaction of DADGEBA and S, which showed an incredible dual-curing behavior that the two functional groups linking in one backbone did not inhibit each other. This finding aroused our great interest because it presented a brand new dual-curing system of epoxy thermosets. Besides, S was the first time reported for the curing agent of epoxy resin [24]. Based on this finding, we speculated that the dual-curing process of DADGEBA/S included two reactions: the crosslinking of double bonds initiated by thiyl radicals and the ring-opening reaction of epoxy groups with thiol groups, which are active functional groups that can react with epoxy groups.

To confirm this speculation, our team had done a great quantity of work. Zhang et al. focused on the curing kinetics of DADGEBA/S by DSC analysis, and the results showed that the curing was a two-stage process, which satisfied two different types of curing kinetic model, respectively [25]. Jia et al. studied on a S/liquid nitrile butadiene rubber (LNBR)/epoxy resin (EP) curing system and found that the S/LNBR/EP system was a two-stage process; besides, NBR and EP formed chemical crosslinking networks [26].

However, previous researchers in our team just confirmed the two-stage curing behavior of the DADGEBA/S system and did not present any direct experimental results to verify the generation of thiol groups in the reaction process. Therefore, the proposed dual-curing mechanism still lacked direct evidence as well as in-depth theoretical discussion. Indeed, it is of great difficulty to detect the intermediate-thiol groups in the DADGEBA/S system even if the thiol groups were produced in the reaction, because they would follow by participating in the ring-opening reaction of epoxy groups. In this paper,

we selected two model compounds: Bisphenol-A diglycidyl ether (BADGE) and 2-Allylphenol (OAP). And we comparatively investigated the reaction of OAP/S, OAP/S/BADGE, and OAP/BADGE systems monitored by FTIR, NMR, NIR, and DSC to provide direct evidence for the dual-curing mechanism of EP/AC/S system through the characterization of thiol groups, conversion rate curve of characteristic groups, and DSC heat analysis. Ultimately, we illustrated and discussed the dual-curing mechanism of EP/AC/S system theoretically.

This work presented a brand new dual-curing mechanism of epoxy thermosets, which not only will enrich the dual-curing system of epoxy resin, but also has theoretical significance for exploiting sulfur and its related sulfur donors as the novel epoxy curing agents.

## Experimental

### Materials

Sulfur (S, purity 99.99 %) was purchased from Aladdin Reagent Co. (Shanghai, China). 2-Allylphenol (OAP, purity 98 %) was obtained from J&K scientific (Beijing, China). Bisphenol-A diglycidyl ether (BADGE, epoxy value 0.51) was purchased from Sinopec Group (Beijing, China).

### Characterization

$^1$H NMR measurement was carried on a Bruker Advance 400 spectrometer (400 MHz) at ambient temperature using Deuterated acetone (contain 0.05 % v/v TMS) as the solvent. The FTIR spectra were recorded on a Bruker Alpha FTIR at a resolution of 4 cm$^{-1}$ in the standard wavenumber range of 4000–400 cm$^{-1}$ using KBr pellets, and the Real-Time Infrared Spectroscopy (RT-FTIR) was conducted to

monitor the conversion rate of characteristic groups using the same instrument, each sample was scanned for 32 times. Near-Infrared Reflection (NIR) spectra of the samples were recorded on a Nicolet Antaris II FT-NIR by accumulating 32 scans at a resolution of 2 cm$^{-1}$ in the wavenumber range of 10000–4000 cm$^{-1}$. Thermal analyses were carried out on a TA Instruments Q20 differential scanning calorimeter (DSC) equipped with an RCS 90 cooling system with the following thermal program (dry N$_2$ was used as the protective atmosphere): OAP/S system was heated from 40 to 275 °C, OAP/S/BADGE system was heated from 40 to 350 °C, and OAP/BADGE system was heated from 40 to 300 °C. Furthermore, individual S was also tested from 40 to 300 °C. All of the above DSC programs were tested at a heating rate of 10 °C/min.

### Reaction procedure

OAP and S (mass ratio 3/1) mixture was charged into a 15 ml vial (using magnetic stirring). Then the reaction mixture was stirred at different temperatures (120/150/160/170/180/190/200 °C) for 30 min. All the as-prepared products were tested by FTIR experiment and compared the degree of reaction. Besides, the 190 °C product was tested by NIR and $^1$H NMR. In addition, neat OAP was stirred at 190 °C for 30 min and tested by $^1$H NMR. The formula of OAP/S system reacted at different temperatures is listed in Table 1.

Furthermore, the OAP/S (mass ratio 3/1) as well as OAP/S/BADGE (mass ratio 3/1/10) system was well mixed for RT-FTIR and DSC tests, while the OAP/BADGE (mass ratio 3/10) system was well mixed only for DSC test. And the RT-FTIR was tested in a special mold, which could hold two KBr window pieces vertically, and the mixture was placed in the middle of the two KBr window pieces. During the experiment, the mold was put in an air-circulating

**Table 1** The formula of OAP/S system reacted at different temperatures and the reaction phenomenon observed by DSC and FTIR

| Temperature (°C) | OAP (g) | S (g) | Phenomenon |
| --- | --- | --- | --- |
| 120 | 3.0016 | 1.0021 | No reaction |
| 150 | 3.0025 | 1.0016 | No reaction |
| 160 | 3.0032 | 1.0009 | No reaction |
| 170 | 2.9988 | 1.0012 | React but thiol group cannot be observed |
| 180 | 3.0028 | 1.0007 | React and thiol group can be observed |
| 190 | 2.9976 | 0.9991 | React and thiol group can be observed |
| 200 | 3.0008 | 1.0014 | React and thiol group can be observed |
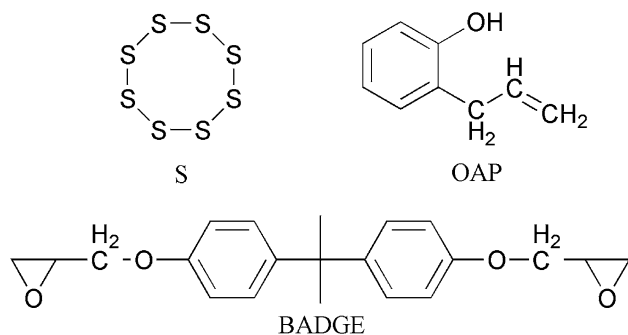
Figure 2 The structure of S, BADGE, and OAP.



Figure 3 DSC curve of sulfur (S).

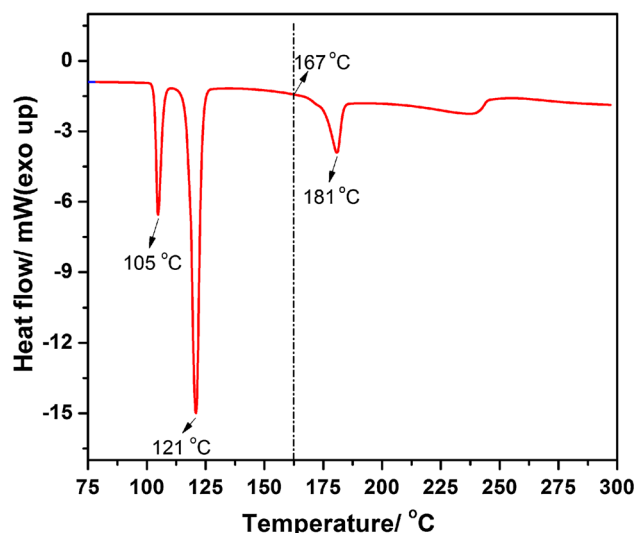oven at 175 °C, and the FTIR spectra were recorded periodically.

It should be noted that the S decomposition is a complicated process, during which the amount of generated thiyl radicals are hard to calculate because of the octatomic ring structure of S as shown in Fig. 2. In this paper, the dosage of S in the OAP/S and OAP/S/BADGE systems is enough to consume the double bonds and epoxy groups completely.

## Results and discussion

### The influence of temperature on the OAP/S reaction

Figure 3 is the DSC curve of S, which has two allotropes: monoclinic S ($S_\beta$) and orthorhombic S ($S_\alpha$). And it was reported that S expressed different allotropes depending on the temperature [27, 28]. In Fig. 3, the peak at 105 °C is attributed to the phase transformation of S from $S_\alpha$ to $S_\beta$, while the peak at 121 °C corresponds to the melting point of S [29]. When the temperature reached about 167 °C, S began to go through a cleavage heat absorption process and the peak temperature was 181 °C. Therefore, it is concluded that the decomposition temperature of S was started at 167 °C, above which thiyl radicals can be produced.

By comparing the FTIR spectra of OAP/S system at different temperatures according to Fig. 4a, it is concluded that the reaction did not happen because the 1640 cm$^{-1}$ peak, which corresponds to the C=C stretching vibration, had little change when the temperature was below 170 °C. However, the 1640 cm$^{-1}$ peak would have greater decrease with the increase of the reaction temperature when the temperature was above 170 °C (including 170 °C).

And, when the temperature was higher than 190 °C (including 190 °C), the absorption peak at 1640 cm$^{-1}$ disappeared within 30 min, which means the allyl double bonds had reacted completely. Moreover, when the temperature was above 180 °C (including 180 °C), a new peak can be observed appearing at 2563 cm$^{-1}$, which is assigned to the S–H stretching vibration of thiol group, as shown in Fig. 4b. And the peak at 2563 cm$^{-1}$ reached the maximum value when the reaction temperature was up to 190 °C. Afterward, we chose the products of OAP/S reacted at 190 °C for further characterization of thiol groups.

To further study the OAP/S reaction, the FTIR spectrum obtained at 190 °C was separately picked out for analyzing, as shown in Fig. 4c. In general, the asymmetrical stretching vibration and the symmetrical stretching vibration of saturated methylene group (CH$_2$) are at 2920 and 2850 cm$^{-1}$, respectively. However, the two bands will move to 2980 and 2900 cm$^{-1}$ when the methylene groups are directly bonded with the double bonds, so it can be seen that the CH$_2$ stretching vibration of OAP moves to 2923 and 2864 cm$^{-1}$ from 2978 and 2907 cm$^{-1}$, respectively, after the reaction of OAP/S. We proposed there are two reasons to explain this phenomenon: one is that the α-H atoms of the allyl group was extracted by the thiyl radicals and formed thiol groups; the other is that the double bonds turned to saturated state owing to the addition reaction with thiyl radicals, as shown in Scheme 3. Therefore, we chose 2980 cm$^{-1}$ as the characteristic peak of
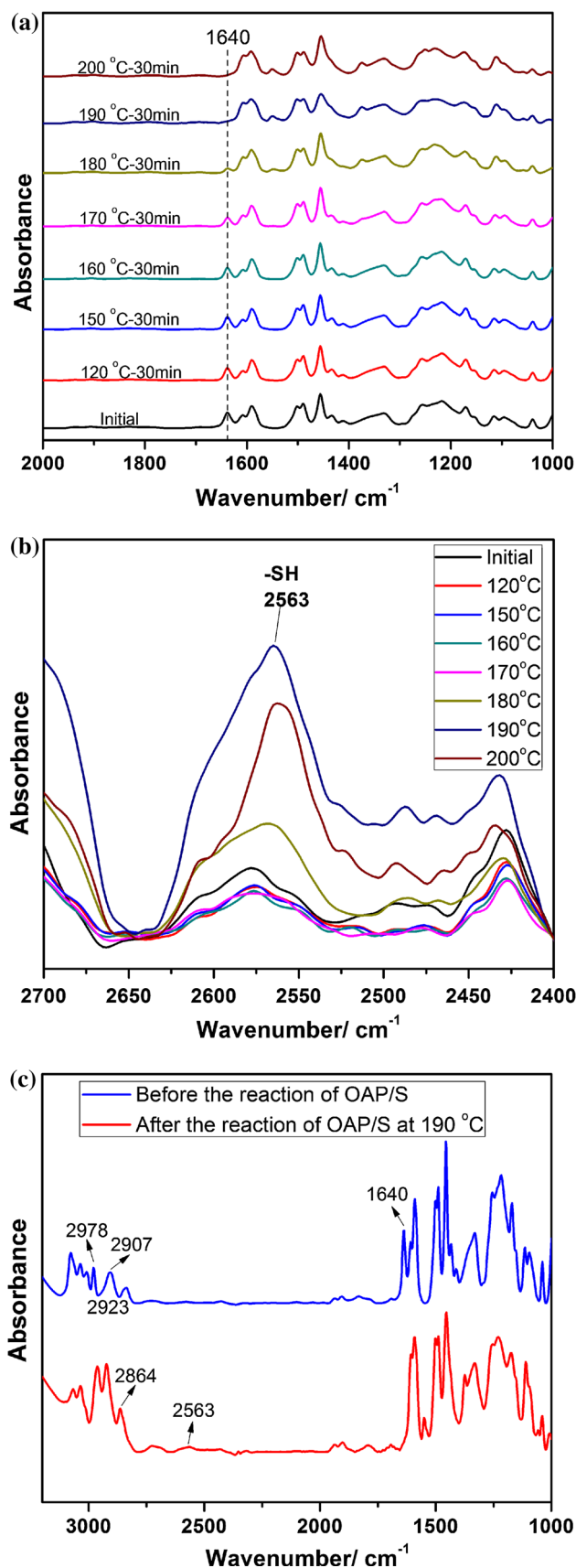
**(a)**

**(b)**

**(c)**

methylene groups in the Real-Time Infrared Spectroscopy (RT-FTIR) of OAP/S system in the latter part of this article. It should be noted that the phenolic hydroxyl may also be attacked by the thiyl radicals, which will be discussed in the latter part of this article.

## The characterization of thiol groups in OAP/ S system

### NIR spectra

Near-infrared light is a kind of electromagnetic wave whose wave number is between visible light and mid-infrared (MIR) light ranging from 4000 to 12800 nm [30]. Recent years, NIR analysis has played an increasingly role and was widely used in the characterization of hydric groups [31, 32]. This implies that it is very feasible to use NIR technic to detect the thiol groups produced in the OAP/S reaction.

Figure 5 is the NIR spectra of OAP/S system before and after the reaction at 190 °C. Before the reaction of OAP/S, the absorption bands around 8754, 8240, 6939, 6115, 5957, and 5670 cm$^{-1}$ are attributed to C–H (in the aromatic structure) second overtone, C–H (in the methylene structure) second overtone, O–H first overtone, C–H (in the vinyl structure) first overtone, C–H (in the aromatic structure) first overtone, and C–H (in the methylene structure) first overtone [33]. Besides, there were two peaks about the C–H combination overtone of vinyl structure at 4720 and 4476 cm$^{-1}$, respectively [33]. After the reaction of OAP/S, the peaks at 4720, 4476, and 6115 cm$^{-1}$ disappeared, by which it can be concluded that allyl double bonds had consumed completely. Moreover, there was a new peak at 5733 cm$^{-1}$, which is attributed to the S–H first overtone [33, 34]. In addition, we had pointed that the α-H atoms of the allyl groups were extracted by the thiyl radicals and formed thiol groups; however, it was observed that the height of 6939 cm$^{-1}$ peak, which is assigned to the phenolic hydroxyl, reduced a little after the reaction. This might be the fact that the
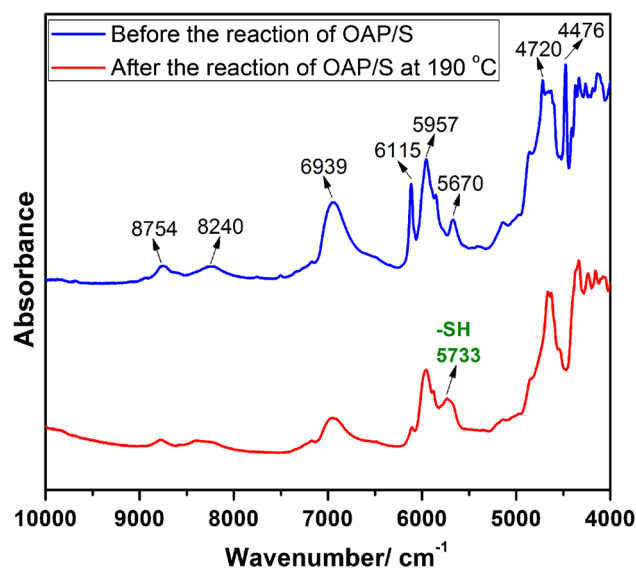
**Figure 5** NIR spectra of OAP/S system before and after the reaction at 190 °C for 30 min.

phenolic hydroxyl was also attacked by the thiyl radicals; nevertheless, the limit change of peak at 6939 cm$^{-1}$ revealed that this is just a side reaction, and would have little influence on the discussion of OAP/S reaction. In conclusion, the double bonds had reacted completely and the thiol groups were generated during the reaction process of OAP/S.

*NMR spectra*

All the chemical shift of basic peaks of OAP had been marked in Fig. 6a, which coincides with the OAP structure well, and i and j are attributed to the peaks of deuterated acetone solvent. It is obvious that the $^1$H NMR spectrum of pure OAP heated at 190 °C for 30 min had little change comparing to that of pure OAP except for some peaks ranging from 2.4 to 1.0 ppm. However, after the reaction of OAP and S, the $^1$H NMR spectrum became much more complicated owing to the multitudinous final products through the coupling reactions among the various radicals generated in this system shown in Scheme 3. The peaks of f and g disappeared, which revealed the complete consumption of double bonds. Besides, it can be concluded that α-H atoms of allyl groups consumed completely because the peak e disappeared after the reaction. Although the final products of this system cannot be figured out, the multiple peaks between 3.0 and 3.5 ppm could be attributed to the as-produced saturated methine protons like –C–
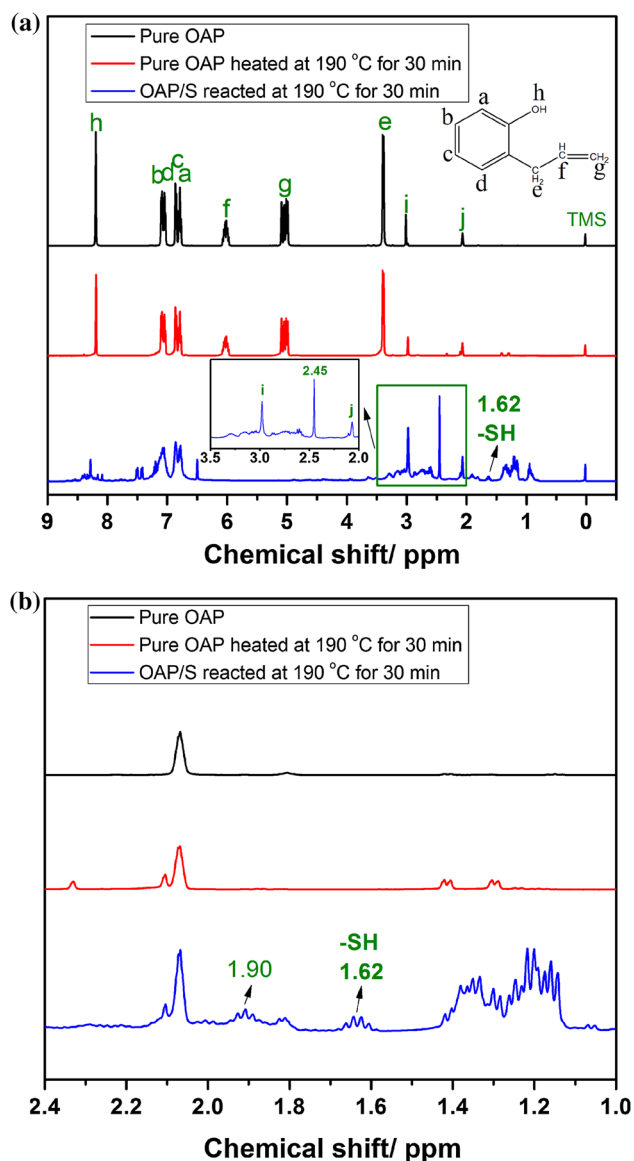


**Figure 6** $^1$H NMR spectra of OAP/S system at 190 °C for 30 min: **a** 9–0 ppm region; **b** 2.4–1.0 ppm region.

C*H*–Ar– and –S–C*H*–Ar–. While the multiple peaks between 3.0 and 2.5 ppm could be assigned to the methylene protons like –C–C*H₂*–Ar–, an apparent peak appearing at 2.45 ppm is most probably the methylene protons of the –C–C*H₂*–S– structure. Moreover, evidence is provided here that thiol groups generated in this reaction because there was a new peak appearing at 1.62 ppm. It is well-known that thiol group is a functional group that contains active hydrogen atom, so the chemical shift of thiol group in the $^1$H NMR has a relatively wide region from 0.9 to 2.5 ppm [35], but the most possible area is around 1.5 ppm [36]. Although there were many

peaks in this area like the peaks around 1.90 ppm and the multiple peaks in the range of 1.4–1.1 ppm, these peaks cannot be regarded as thiol groups because the peaks around 1.90 ppm could be attributed to the methine protons of the –C–C*H*–C–S– structure, while the peaks in the range of 1.4–1.1 ppm could be the amounts of methine protons of the –C–C*H*–C– structure and methylene protons of the –C–C*H*$_2$–C– structure. Moreover, it can also be observed that the content of phenolic hydroxyl decreased but did not disappear, which is consistent with the results of NIR spectra. In conclusion, both the double bonds and the α-H atoms of allyl groups consumed completely, and thiol groups were generated during the process of OAP/S reaction.

## The comparison of OAP/S and OAP/S/BADGE

### RT-FTIR analysis

Real-Time Infrared Spectroscopy (RT-FTIR) was collected to record the change of methylene groups, double bonds, and epoxy groups by monitoring peaks at 2978, 1640, and 915 cm$^{-1}$, respectively. And the degree of conversion was calculated as

$$\alpha(t) = 1 - \frac{A(t)_i / A(t)_{1500}}{A(0)_i / A(0)_{1500}}, \tag{1}$$

where $\alpha(t)$ is the degree of conversion of characteristic group at $t$ time, $A(t)_i$ is the area of $i$ group at $t$ time, $A(0)_i$ is the area of $i$ group at the beginning, $A(t)_{1500}$ is the area of benzene at t time, and $A(0)_{1500}$ is the area of benzene at the beginning. It has been known that the reaction temperature of OAP/S should be above 170 °C in the former part, while the reaction rate will be too fast to monitor the degree of conversion of characteristic groups if the temperature is too high. For instance, it was seen that both the 2978 and 1640 cm$^{-1}$ had disappeared in 30 min when the reaction temperature is 190 °C, as shown in Fig. 5. Besides, phenolic hydroxyl of OAP can react with the epoxy group without base catalyst around 200 °C [2]. Therefore, the RT-FTIR experiments of the OAP/S and OAP/S/BADGE systems were carried out at 175 °C, which is an appropriate temperature to avoid side reactions and collect the data accurately.

Figure 7 is the conversion rate curve of OAP/S reacted at 175 °C. We had mentioned that the OAP/S system exhibited two reactions: one is that the α-H
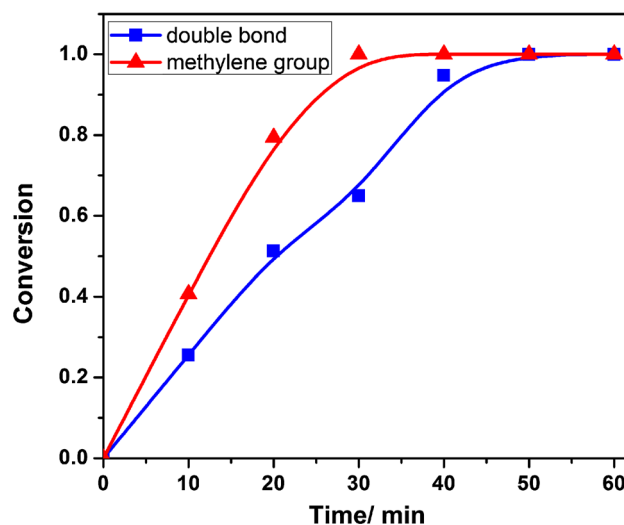


**Figure 7** The reaction time dependence of conversion rate of double bond and methylene group in OAP/S system reacted at 175 °C.

atoms of the allyl group was extracted by the thiyl radicals and formed thiol groups; the other is that the double bonds turned to saturated state owing to the addition reaction with thiyl radicals. Therefore, the conversion rate of methylene group was used to estimate the former process, while the conversion rate of double bond was used to measure the latter reaction. The results showed that the reaction rate of the former process was faster than that of the latter one, that is, the reaction of generation of thiol groups played the dominant role in the OAP/S reaction.

Figure 8 is the relationship of conversion rate of OAP/S/BADGE reacted at 175 °C, and reaction time and degree of conversion were also calculated by the Eq. (1). The data showed that both the double bond and epoxy group consumed at a very fast speed at the initial stage. However, it should be noted that 915 cm$^{-1}$ was selected as the monitored area of epoxy group, and the CH$_2$ out-of-plane bending vibration of double bond also appeared at the same area. Therefore, the red curve is the combined conversion rate of epoxy group and double bond. Nevertheless, in the OAP/S/BADGE system, the content of double bond was much less than that of epoxy group, which would have no reactions until the allyl double bonds began to react and produce thiol groups. Besides, we can see that double bonds consumed completely in 50 min, while the conversion rate of epoxy group reached 100 % in 400 min. Consequently, the red curve was the summation of the consumptions of
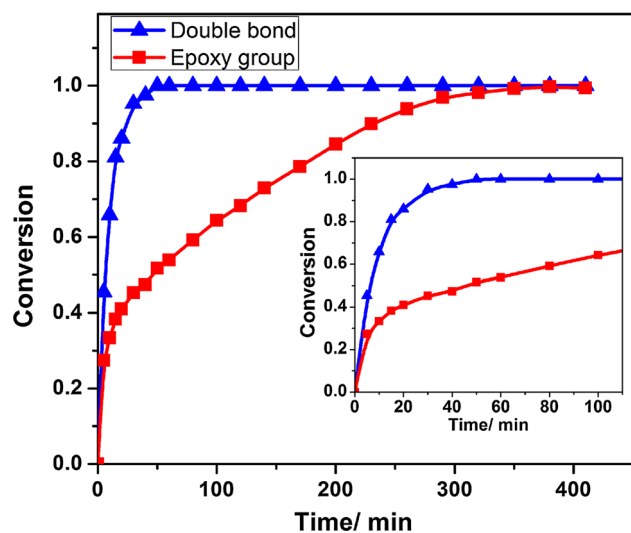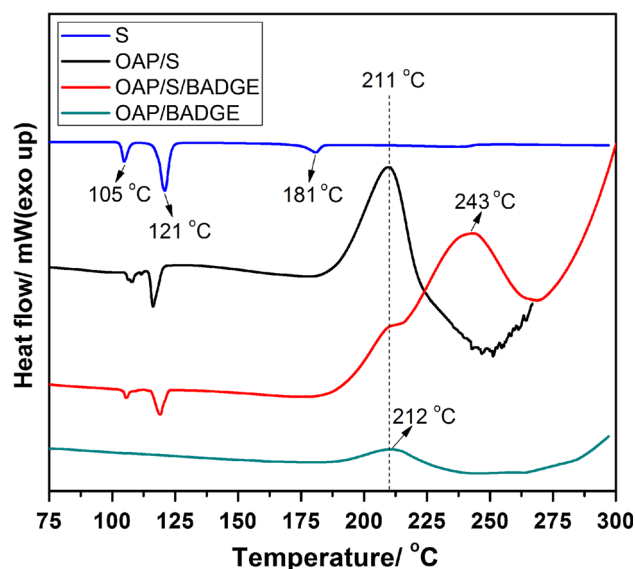
**Figure 8** The reaction time dependence of conversion rate of double bond and epoxy group in OAP/S/BADGE system reacted at 175 °C.



**Figure 9** DSC curves of S, OAP/S, OAP/S/BADGE, and OAP/BADGE systems.

epoxy groups as well as double bonds at the initial 50 min but mainly was double bonds, while it only represented the conversion rate of epoxy group after 50 min because the double bonds had consumed completely at this time. And thus, we can observe that the conversion rate of epoxy group exhibited a quick consumption in the first 50 min, after which epoxy group remained a slow but average consumption rate in a very long time. The fact that double bond and epoxy group disappeared sequentially was consistent with the proposed dual-curing mechanism, as shown in Scheme 3.

*DSC analysis*

DSC scans were collected on four different systems: S, OAP/S, OAP/S/BADGE, and OAP/BADGE. According to Fig. 9, two endothermic peaks around 105 and 121 °C can be seen in all of the curves except for OAP/BADGE, which are due to the phase transition of S from $S_\alpha$ to $S_\beta$ and the melting of S, respectively. Then, it can be concluded that S had completely split into thiyl radicals because of the third endothermic peak at 181 °C, which is also the starting temperature of the exothermic process in both the OAP/S and OAP/S/BADGE systems. Therefore, the exothermic process from 181 to 211 °C is due to the reaction of thiyl radicals with allyl double bonds. The second exothermic process around 243 °C can be seen in the OAP/S/BADGE

system, which could only be attributed to the ring-opening reaction of epoxy groups and thiol groups, and these thiol groups are produced by the reaction of thiyl radicals and allyl double bonds at the temperature from 181 to 211 °C. Moreover, the DSC curve of OAP/BADGE experienced a weak exothermic reaction around 212 °C, which suggested that phenolic hydroxyl could react with epoxy groups at high temperature, but the ring-opening reaction of epoxy groups of OAP/S/BADGE mainly depends on the thiol groups. In conclusion, the one-stage reaction of OAP/S and the two-stage reaction of OAP/S/BADGE perfectly followed the proposed dual-curing mechanism, as shown in Scheme 3.

**Proposed dual-curing mechanism**

To obtain an accurate path way for the dual-curing process of EP/AC/S system, we referenced the mechanism of S vulcanization as well as the mechanism of thiol-ene click chemistry.

Actually, the reactions of S with compounds containing double bond are certainly not a recent discovery. Dating back to the middle of the 1900s, Charles Goodyear, an American chemist, had discovered that natural rubber (poly(cis-isoprene)) could be vulcanized by S [37]. Since then, S has been widely used to crosslink polymers. Meanwhile, the mechanism of S vulcanization [38] was highly discussed; however, until now, the mechanism is still

not completely understood in the academic world. At present, there are mainly two standpoints on the vulcanization mechanism, one is free radical mechanism, and the other is ionic mechanism. There is also a saying that the vulcanization is proceeding in mixed mechanisms simultaneously or successively [39, 40]. According to the explanation of free radical mechanism, the S vulcanization is a process that crosslinking networks are formed among rubber molecules by the reaction between double bonds in rubber and thiyl radicals, which are generated by homolytic cleavage of S. During this process, the thiyl radicals will extract the α-H atoms of allyl groups to generate thiol groups and produce crosslinking active position. The radical mechanism of vulcanization is shown in Scheme 1 [41].

The vulcanization process of rubber is also the birth of one of the most significant click chemistry [42] type: thiol-ene reaction, which was highlighted and studied by countless researchers and several reviews had been published in the past few years [43–45]. The addition of thiols across unsaturated carbon–carbon double bonds can take place by the Michael-type nucleophilic addition [46] mechanism or classical radical addition [47] mechanism. In general, the Michael-type nucleophilic addition should satisfy two conditions: first of all, the carbon–carbon double bonds should be electron-deficient type; secondly, the chemical reaction needs to be initiated by base or nucleophile catalysts [46]. However, neither of the above conditions can be met in the OAP/S/BADGE system. Therefore, it is impossible for the Michael-type nucleophilic addition to occur. In contrast, the dual-curing mechanism of Epoxy (EP)/Allyl Compound (AC)/S system can reference the free radical chain mechanism of thiol-ene system, which is shown in Scheme 2: a radical produced by initiator under heating or lighting conditions abstracts a hydrogen atom from a thiol monomer and produced a thiyl radical, which can follow to participate in the addition reaction with double bonds and generate new radical active center, and then the radical active center can abstract a hydrogen atom from a thiol monomer, during which the new thiyl radicals are generated and can further take part in the addition reaction with the double bonds according to Step 2. In this case, the reaction can proceed continuously [47].

Based on the traditional free radical mechanism of S vulcanization and the radical addition mechanism of thiol-ene reaction, we proposed the whole process
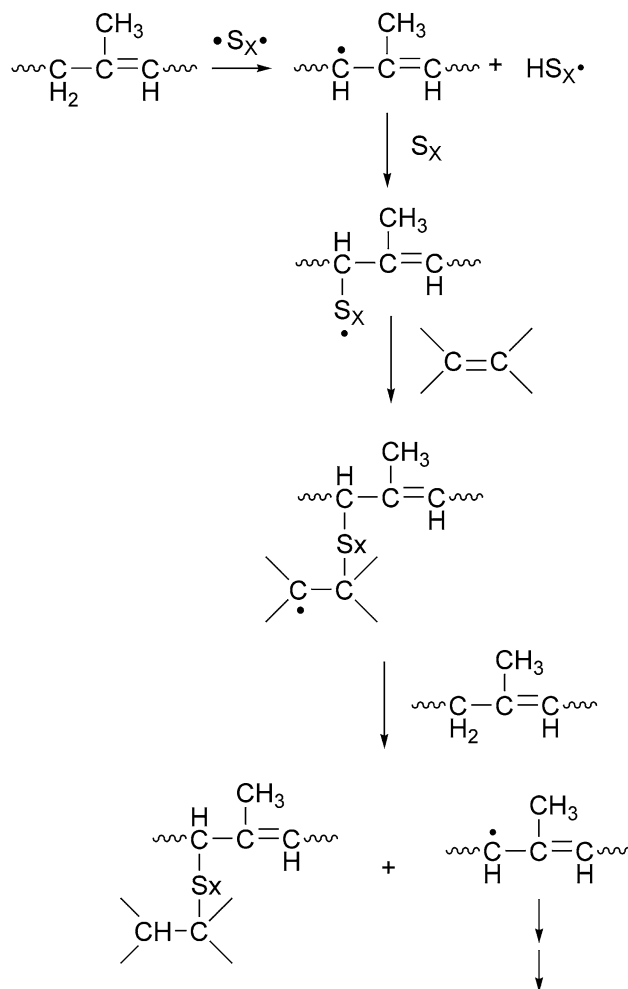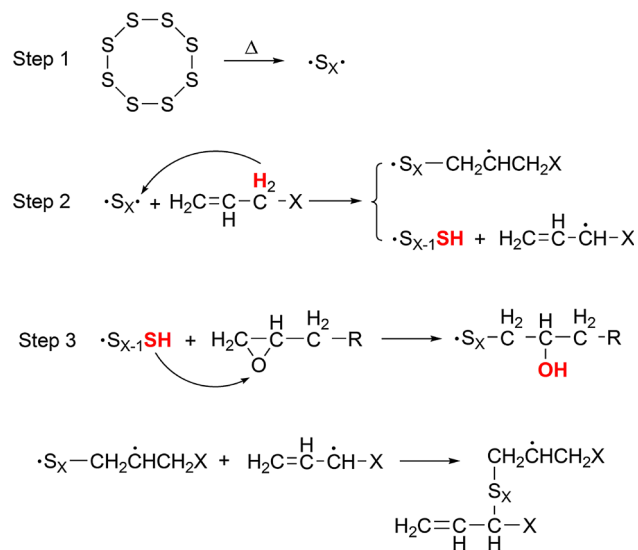


Scheme 1 Radical mechanism of sulfur (S) vulcanization.
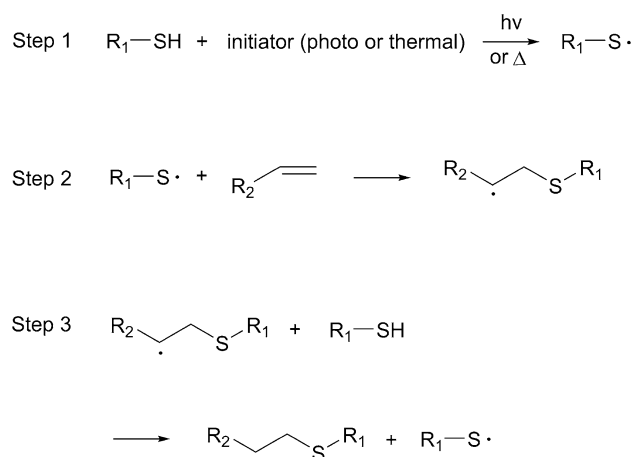


Scheme 2 Free radical chain mechanism of thiol-ene system.

of the dual-curing mechanism of EP/AC/S system shown in Scheme 3. Firstly, thiyl radicals are generated through sulfur cleavage at high temperature. Secondly, there exists two reaction routes: one is thiyl

**Scheme 3** Proposed dual-curing mechanism of EP/AC/S system.

radicals capture α-H atoms from allyl groups to form thiol groups and the radicals transfer to the allyl structure; the other is thiyl radicals participate in an addition reaction with double bonds. Thirdly, the epoxy ring-opening reaction occurs via the reaction with thiol groups; meanwhile, all of the radicals generated in the previous steps take part in the terminal reactions by radical–radical coupling.

## Conclusion

EP/AC/S system, which possesses a unique curing mechanism, is a facile and novel dual-curing system that consists of the crosslinking of double bonds initiated by thiyl radicals and the ring-opening reactions of epoxy groups with thiol groups. S cleaves to form thiyl radicals above 170 °C and thiol groups can be generated in the reaction of OAP/S system, which provides direct evidence for the dual-curing mechanism of EP/AC/S system. Furthermore, DSC and RT-FTIR data are consistent with the dual-curing mechanism of EP/AC/S system, which shares a close resemblance to the classical rubber vulcanization mechanism and the recent thiol-ene radical addition mechanism. However, the reaction of EP/AC/S system is of great complicacy owing to the complex reaction of double bonds with thiyl radicals, and the accurate structure of the final products of this system is quite difficult to figure out. Further studies can focus on this issue and make the dual-curing mechanism of EP/AC/S system more clearly and easily

understood. And more S donor systems can be studied to enrich this dual-curing system. In conclusion, the clarification of the dual-curing mechanism of EP/AC/S system greatly enriches the dual-curing system of epoxy thermosets, and thus provides a significant thought to prepare unique adhesives for a wide range of applications, for example, improving the adhesion between rubber and metal.

## Acknowledgements

## References

[1] May C (1987) Epoxy resins: chemistry and technology. CRC Press, Boca Raton

[2] Ellis B (1993) Chemistry and technology of epoxy resins. Springer, New York

[3] Gu R, Sain M, Konar S (2014) Development and characterization of flexible epoxy foam with reactive liquid rubber and starch. J Mater Sci 49(8):3125–3134

[4] Zhang C, Myers JN, Chen Z (2014) Molecular behavior at buried epoxy/poly(ethylene terephthalate) interface. Langmuir 30(42):12541–12550. doi:10.1021/la502239u

[5] Silva LC, Silva GG, Ajayan PM, Soares BG (2015) Long-term behavior of epoxy/graphene-based composites determined by dynamic mechanical analysis. J Mater Sci 50(19):6407–6419

[6] Min Y, Huang S, Wang Y, Zhang Z, Du B, Zhang X, Fan Z (2015) Sonochemical transformation of epoxy–amine thermoset into soluble and reusable polymers. Macromolecules 48(2):316–322. doi:10.1021/ma501934p

[7] Naumann S, Speiser M, Schowner R, Giebel E, Buchmeiser MR (2014) Air stable and latent single-component curing of epoxy/anhydride resins catalyzed by thermally liberated N-heterocyclic carbenes. Macromolecules 47(14):4548–4556. doi:10.1021/ma501125k

[8] Petrie E (2006) Epoxy adhesive formulations. McGraw-Hill, New York

[9] Pascault J-P, Williams RJ (2009) Epoxy polymers. Wiley, Weinheim

[10] Lee SW, Park JW, Park CH, Lim DH, Kim HJ, Song JY, Lee JH (2013) UV-curing and thermal stability of dual curable urethane epoxy adhesives for temporary bonding in 3D multi-chip package process. Int J Adhes Adhes 44:138–143

[11] Park YJ, Lim DH, Kim HJ, Park DS, Sung IK (2009) UV- and thermal-curing behaviors of dual-curable adhesives

based on epoxy acrylate oligomers. Int J Adhes Adhes 29(7):710–717

[12] Guzmán D, Ramis X, Fernández-Francos X, Serra A (2015) Preparation of click thiol-ene/thiol-epoxy thermosets by controlled photo/thermal dual curing sequence. RSC Adv 5(123):101623–101633

[13] Gadwal I, Stuparu MC, Khan A (2015) Homopolymer bifunctionalization through sequential thiol–epoxy and esterification reactions: an optimization, quantification, and structural elucidation study. Polym Chem 6(8):1393–1404

[14] Jian Y, He Y, Sun Y, Yang H, Yang W, Nie J (2013) Thiol–epoxy/thiol–acrylate hybrid materials synthesized by photopolymerization. J Mater Chem C 1(29):4481–4489

[15] Westover AS, Baer B, Bello BH, Sun H, Oakes L, Bellan LM, Pint CL (2015) Multifunctional high strength and high energy epoxy composite structural supercapacitors with wet-dry operational stability. J Mater Chem A 3(40): 20097–20102

[16] Huang K, Liu Z, Zhang J, Li S, Li M, Xia J, Zhou Y (2014) Epoxy monomers derived from tung oil fatty acids and its regulable thermosets cured in two synergistic ways. Biomacromolecules 15(3):837–843

[17] Ortiz RA, Valdéz AEG, Duarte LB, Santos RG, Flores LRO, Soucek MD (2008) Development and study of a coupling agent for photocurable hybrid thiol/ene/cationic formulations. Macromol Chem Phys 209(20):2157–2168

[18] Foix D, Ramis X, Serra A, Sangermano M (2011) UV generation of a multifunctional hyperbranched thermal crosslinker to cure epoxy resins. Polymer 52(15):3269–3276

[19] Kim J, Oh H, Kim E (2008) A dual-functional monomer having an epoxy and methacrylate group for holographic recording. J Mater Chem 18(40):4762–4768

[20] Martin RW, Pannell CE (1960) Ethers of epoxy-substituted phenols and their polymers. Google Patents, Mountain View

[21] Ursache O, Gaina C, Gaina V, Musteata VE (2012) High performance bismaleimide resins modified by novel allyl compounds based on polytriazoles. J Polym Res 19(10):1–9

[22] Meng J, Hu X, Boey FYC, Li L (2005) Effect of layered nano-organosilicate on the gel point rheology of bismaleimide/diallylbisphenol A resin. Polymer 46(8): 2766–2776. doi:10.1016/j.polymer.2004.11.087

[23] Qin H, Mather PT, Baek JB, Tan LS (2006) Modification of bisphenol-A based bismaleimide resin (BPA-BMI) with an allyl-terminated hyperbranched polyimide (AT-PAEKI). Polymer 47(8):2813–2821. doi:10.1016/j.polymer.2006.02.062

[24] Zhang J, Huang H, Liu L (2004) Curing reaction of DAD-GEBA with sulfur. Beijing Univ Chem Technol Nat Sci Ed 31(3):59–61

[25] Zhang G, Cheng J, Shi L, Lin X, Zhang J (2012) Study on curing kinetics of diallyl-bearing epoxy resin using sulfur as

curing agent. Thermochim Acta 538:36–42. doi:10.1016/j.tca.2012.03.012

[26] Jia C, Li T, Cheng J, Zhang J (2015) The curing mechanism of epoxy resin/liquid nitrile rubber system by sulfur and its network structure. Acta Polym Sin 12:1377–1386

[27] Bordoloi BK, Pierce EM (1978) Plastic sulfur stabilization by copolymerization of sulfur with dicyclopentadiene. Adv Chem Ser 165:31–53

[28] Bourne DJ (1978) New uses of sulfur, II: a symposium, vol 165. Amer Chemical Society, New York

[29] Liu Y, Wang T, Qin L, Jin Y (2008) Urea particle coating for controlled release by using DCPD modified sulfur. Powder Technol 183(1):88–93

[30] McClure WF (2003) 204 years of near infrared technology: 1800–2003. J Near Infrared Spectrosc 11(6):487–518

[31] Manley M (2014) Near-infrared spectroscopy and hyperspectral imaging: non-destructive analysis of biological materials. Chem Soc Rev 43(24):8200–8214. doi:10.1039/c4cs00062e

[32] Pansare VJ, Hejazi S, Faenza WJ, Prud'homme RK (2012) Review of long-wavelength optical and NIR imaging materials: contrast agents, fluorophores, and multifunctional nano carriers. Chem Mater 24(5):812–827

[33] Workman J Jr, Weyer L (2007) Practical guide to interpretive near-infrared spectroscopy. CRC Press, Boca Raton

[34] Li J, Zhang Y, Cai W, Shao X (2011) Simultaneous determination of mercury, lead and cadmium ions in water using near-infrared spectroscopy with preconcentration by thiol-functionalized magnesium phyllosilicate clay. Talanta 84(3):679–683. doi:10.1016/j.talanta.2011.01.072

[35] Chamberlain N (1974) The practice of NMR spectroscopy. Springer, New York

[36] Zhao B, Zheng Y, Weng Z, Cai S, Gao C (2015) The electrophilic effect of thiol groups on thiol–yne thermal click polymerization for hyperbranched polythioether. Polym Chem 6(20):3747–3753. doi:10.1039/c5py00307e

[37] Posner T (1905) Beiträge zur Kenntniss der ungesättigten Verbindungen. II. Ueber die Addition von Mercaptanen an ungesättigte Kohlenwasserstoffe. Ber Dtsch Chem Ges 38(1):646–657

[38] Lewis W, Squires L, Nutting RD (1937) Mechanism of rubber vulcanization with sulfur. Ind Eng Chem 29(10):1135–1144

[39] Krejsa M, Koenig J (1993) A review of sulfur crosslinking fundamentals for accelerated and unaccelerated vulcanization. Rubber Chem Technol 66(3):376–410

[40] Dondi D, Buttafava A, Zeffiro A, Palamini C, Lostritto A, Giannini L, Faucitano A (2015) The mechanisms of the sulphur-only and catalytic vulcanization of polybutadiene: an EPR and DFT study. Eur Polym J 62:222–235. doi:10.1016/j.eurpolymj.2014.11.012

[41] Hou Y, You C (2013) Rubber vulcanization. Chemical industry press, Beijing

[42] Kolb HC, Finn M, Sharpless KB (2001) Click chemistry: diverse chemical function from a few good reactions. Angew Chem Int Ed 40(11):2004–2021

[43] Dondoni A, Marra A (2012) Recent applications of thiol–ene coupling as a click process for glycoconjugation. Chem Soc Rev 41(2):573–586

[44] Kade MJ, Burke DJ, Hawker CJ (2010) The power of thiol-ene chemistry. J Polym Sci Part A Polym Chem 48(4):743–750

[45] Hoyle CE, Lowe AB, Bowman CN (2010) Thiol-click chemistry: a multifaceted toolbox for small molecule and polymer synthesis. Chem Soc Rev 39(4):1355–1387

[46] Nair DP, Podgórski M, Chatani S, Gong T, Xi W, Fenoli CR, Bowman CN (2013) The thiol-Michael addition click reaction: a powerful and widely used tool in materials chemistry. Chem Mater 26(1):724–744

[47] Hoyle CE, Bowman CN (2010) Thiol–ene click chemistry. Angew Chem Int Ed 49(9):1540–1573